Journal of Biomechanics 82 (2019) 109–115

Contents lists available at ScienceDirect

Journal of Biomechanics

journal homepage: www.elsevier.com/locate/jbiomech
www.JBiomech.com

An *in vitro* model quantifying the effect of calcification on the tissue–stent interaction in a stenosed aortic root

Orla M. McGee [a], Wei Sun [b], Laoise M. McNamara [a,*]

[a] MMDRG, Biomechanics Research Centre, Biomedical Engineering, College of Engineering & Informatics, National University of Ireland Galway, Ireland
[b] Wallace H. Coulter Department of Biomedical Engineering, Georgia Institute of Technology, USA

ARTICLE INFO

Article history:
Accepted 17 October 2018

Keywords:
Transcatheter aortic valves
Self-expanding
Radial force
Biomechanics
Aortic stenosis
Tissue-stent interaction

ABSTRACT

Transcatheter Aortic Valves rely on the tissue-stent interaction to ensure that the valve is secured within the aortic root. Aortic stenosis presents with heavily calcified leaflets and it has been proposed that this calcification also acts to secure the valve, but this has never been quantified. In this study, we developed an *in vitro* calcified aortic root model to quantify the role of calcification on the tissue-stent interaction. The *in vitro* model incorporated artificial calcifications affixed to the leaflets of porcine aortic heart valves. A self-expanding nitinol braided stent was deployed into non-calcified and artificially calcified porcine aortic roots and imaged by micro computed tomography. Mechanical tests were then conducted to dislodge the stent from the aortic root and it was found that, in the presence of calcification, there was a significant increase in pullout force (8.59 ± 3.68 N vs. 2.84 ± 1.55 N $p = 0.045$), stent eccentricity (0.05 ± 0.01 vs. 0.02 ± 0.01, $p = 0.049$), and coefficient of friction between the stent and aortic root (0.36 ± 0.12 vs. 0.09 ± 0.05, $p = 0.018$), when compared to non-calcified roots. This study quantifies for the first time the impact of calcification on the friction between the aortic tissue and transcatheter aortic valve stent, showing the role of calcification in anchoring the valve stent in the aortic root.

1. Introduction

Transcatheter Aortic Valve Implantation (TAVI) is a minimally invasive alternative to surgical heart valves in the treatment of aortic stenosis. Since the first implantation in 2002, TAVI procedures have become increasingly popular (Cribier et al., 2002) in particular for patients that are too high risk for surgical heart valve replacements. TAVI has shown favourable hemodynamics and reduced hospitalization and death in such patients (Leon et al., 2010). However, there are potential complications of TAVI implantation, including interference with the mitral valve, interference with the hearts conductance system, paravalvular leakage, reduced device durability and dislodgement of the transcatheter valve into the left ventricle (Block, 2010; Généreux et al., 2013; Masson et al., 2009; Vahanian et al., 2008). The tissue-stent interaction is particularly important for the successful deployment and post-operative device performance for TAVs. It has previously been shown that excessive radial force can lead to aortic root rupture (Wang et al., 2015), whereas inadequate radial force can lead to problems such as migration of the stent into the left ventricle (Dwyer et al., 2009).

Previous studies have computationally investigated the biomechanical interaction between the aortic root and the valve stent (Auricchio et al., 2014; Capelli et al., 2012; Dwyer et al., 2009; Gunning et al., 2014; McGee et al., 2018; Morganti et al., 2016; Morganti et al., 2014; Schoenhagen et al., 2011; Sturla et al., 2016; Sun et al., 2010; Tzamtzis et al., 2013; Wang et al., 2015; Wang et al., 2012). Computational fluid dynamics has been applied to investigate stent migration forces and it has been reported that the antegrade force (0.602 N) is ten times smaller than the retrograde force (6.01 N), and also that the dynamic pressure gradient is the largest contributor to the migration force experienced by TAVs (Dwyer et al., 2009). Similar axial force values (5.8–6.1 N) were predicted to occur under a static diastolic pressure on the leaflets of a 23 mm TAV, with eccentricities of 0.3, 0.5 and 0.68, using finite element analysis (Sun et al., 2010). Numerical analysis has been applied to investigate the force exerted by different TAVI designs on the annulus and it has been shown that the hoop forces of the 26 mm CoreValve vary from 2 to 7 N, for aortic annuli ranging from 20 to 23 mm and that the 26 mm Edwards Sapien has a hoop force of 12–14 N when deployed in a 22 mm aortic annulus of varying stiffness (Tzamtzis et al., 2013). The tissue-stent

* Corresponding author.
E-mail address: laoise.mcnamara@nuigalway.ie (L.M. McNamara).

https://doi.org/10.1016/j.jbiomech.2018.10.010
0021-9290/

interaction has been quantified experimentally *in vitro* using ovine and porcine aortic roots by measuring the radial expansion force of the TAVI stent, the associated annulus deformation, the axial stent pullout force and the coefficient of friction (Mummert et al., 2013). It was reported that the radial force increased by 30–40 % when crimped at body temperature versus room temperature, the coefficient of friction between the TAV and aortic root was found to be 0.10 ± 0.01, and that a minimum dilation of the aortic root of 2.5 mm caused by a radial expansion force of 60 N was required to prevent the stent dislodging into the left ventricle (Mummert et al., 2013). However, these studies did not incorporate leaflet calcification or calcification of the stenotic aortic root and so the impact of calcification on the biomechanical interaction was not taken into account.

The degree of aortic calcification has clinically been shown to predict paravalvular leak, aortic regurgitation and procedural complications (Haensig and Rastan, 2012; Leber et al., 2013; Reinders et al., 2015). Recent computational studies have included calcification when investigating the tissue-stent interaction (Morganti et al., 2016; Morganti et al., 2014; Russ et al., 2013; Sturla et al., 2016; Wang et al., 2015; Wang et al., 2012). A finite element model of a patient-specific stenotic aortic valve was developed to investigate the biomechanical interaction between a TAVI stent and the tissue, and it was reported that calcium deposits elevated stress during TAV stent deployment with peak stresses and strains observed in the calcified regions. These results suggest that calcification helps secure the stent in position (Wang et al., 2012). Using a patient-specific finite element modelling approach Russ et al examined stent deformation when calcification was present versus excluded from the model. The results were then compared to post-operative data of Corevalve stent deformation. The model demonstrated the importance of calcification in the dynamics of stent expansion and the tissue interaction, particularly the quantitative prediction of tissue stress (Russ et al., 2013). It has also been shown that stent deformation known as "dog-boning", whereby the stent exhibits larger expansion at distal portions, is dependent on specific calcification patterns, and leads to localised gaps between the stent and tissue, and higher stress in the region of the calcifications (Sturla et al., 2016). These studies highlight the need to understand the role of calcification for the tissue-stent interaction of TAVs. However, there is a lack of experimental data to validate these models. For this reason, the objective of this study is to develop a calcified *in vitro* model using artificially calcified porcine aortic roots to investigate the effect of leaflet calcification on the tissue-stent interaction and its role in securing the stent in the aortic root.

2. Materials and methods

2.1. Stent radial expansion experiment

A 0.0225″ nitinol wire was used to create a braided stent, with 4 axial and 11 circumferential cells, of 27 mm diameter and height 14 mm (Fig. 1). The stent was made and annealed at 500 °C for 30 min. Based on a previously developed technique (Mummert et al., 2013), a stent crimp experiment was performed on the nitinol braided stent. This was performed by wrapping a vinyl strap around the stent. The strap was mounted onto a uniaxial testing apparatus with one end clamped and fastened between two stainless steel plates, and a narrow slit allowed the strap to be pulled and clamped evenly at the opposite end (Fig. 2). The fixture displacement was used to measure the stent diameter. The hoop force exerted from the strap was measured by a load cell that was attached to a uniaxial machine. The experiments were conducted at 37 °C.

The hoop force was then used to calculate the radial expansion force using the equation Mummert et al. (2013):

$$F_{radial} = 2.\pi F_{hoop} \quad (1)$$

2.2. Root – Stent interaction experiment

Artificial calcifications were created using methods adapted from Wendt et al (Wendt et al., 2009). Commercially available reagents with similar properties to native calcifications were used to make a solution from bone glue (collagen) (Liberon Limited, UK) mixed with water (1:7) and then dissolved, 0.25 g hydroxyl-apatite (Fisher Scientific Company LLC, USA) and 1.75 g calcium carbonate (Fisher Scientific Company LLC, USA). The mixture was dried for 48 h and then fragmented using a scissors, scalpel and by hand. The calcification was first shattered into different sized pieces, which were then weighed and based on the weight the calcification was further cut to the correct weight using a scalpel or scissors to create small equally sized pieces. Using micro Computed Tomography (μCT) (Scanco μCT100) evaluations were performed on the calcifications created in this study and they were found to have Hounsfield Units (HU) of 535+, which is within in the range of that of *in vivo* calcifications (Seiffert et al., 2016).

Porcine hearts were obtained fresh and stored in a −80 °C freezer. Prior to carrying out the experiment, each heart was stored at room temperature for 20 min before being placed in a 37 °C water bath until the heart had defrosted (Mummert et al., 2013). The

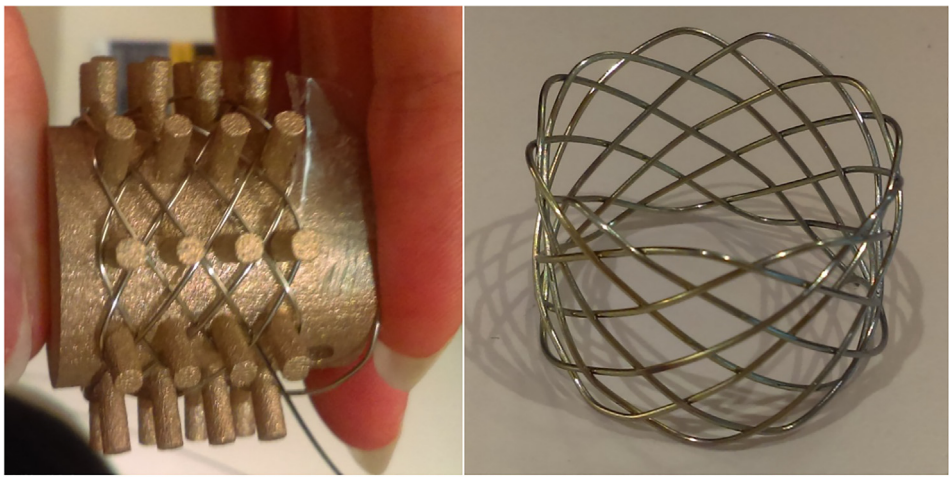

Fig. 1. (a) Braiding of the stent on mandrel (b) finished stent geometry.

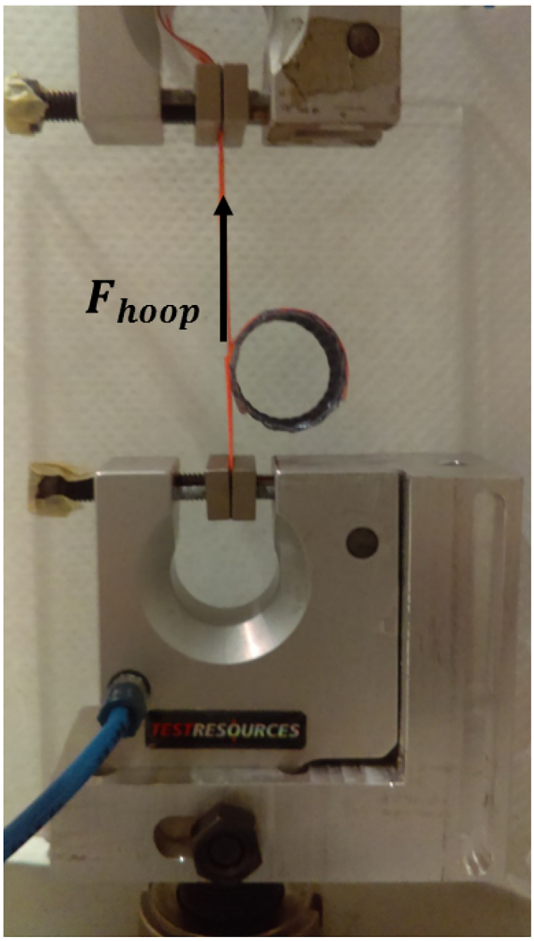

Fig. 2. Radial Force Test.

annulus size of the heart was then measured using an aortic sizer (Medtronic PLC). Using the Agatston scoring method, it was determined that 300 mm^3 of calcification would represent a severe case of calcification. This 300 mm^3 of calcification was attached using cyanoacrylate glue to the leaflets of the aortic valve of porcine hearts, with 19 mm diameter aortic annuli (n = 4) (Fig. 3). A control group of hearts with 19 mm diameter aortic annuli (n = 3) were used without the addition of calcifications. The hearts were then submerged in a 37 °C phosphate buffer saline solution for the duration of the experiment.

For both the calcified and non-calcified groups the specimens were subjected to preconditioning using a valvuloplasty balloon (BARD Peripheral Vascular, Inc., Tempe, AZ) 1 mm larger than the initial diameter for 10 cycles. The stent was then implanted into the aortic root by hand by stretching the stent into a crimped position and then releasing once the valve was implanted so that an equal distribution of the stent was above and below the annulus. The stent was then post dilated to ensure that the stent was under the same loading conditions as the radial force test (Mummert et al., 2013). Evaluations were performed using μCT (μCT100, Scanco) at a resolution of 36.8 μm. Dicom images were exported to Mimics 14.1 Imaging Software (Materialise, Leuven, Belgium) allowing for 3D reconstruction of the stent geometry. Using this reconstructed geometry the dimensions of the stent at the top, middle and bottom were measured (Fig. 4). The eccentricity of the valve stent was measured using the equation (Gooley et al., 2015):

$$e = 1 - \frac{D_{min}}{D_{max}} \tag{2}$$

where D_{max} and D_{min} are the major and minor axes of the ellipse respectively and zero is the optimal eccentricity. The radial force was calculated using the final diameter of the stent and the experimental data.

The pull out force of the stent was measured. This was done by dissecting off the apex of the heart and attaching stiff strings to the end of the stent and to a uniaxial test machine. A constant speed of 20 mm min^{-1} was applied to pull the stent in the direction of the apex (Fig. 5). The pull out force required to pull out the stent was then measured. Using Amontons Coulombs friction law (Mummert et al., 2013; Vad et al., 2010), the pullout force ($F_{pullout}$) can be defined by:

$$F_{pullout} = \mu F_{radial} \tag{3}$$

where μ is the coefficient of friction between the stent and the aortic root and F_{radial} is the radial force exert by the stent on the aortic root.

Using the equation for the *invivo* pull out force (Mummert et al., 2013):

$$F_{in\ \ vivo} = \Delta P_{stent} \pi \left(\frac{d}{2}\right)^2_{stent} \tag{4}$$

we can determine whether the stent would migrate into the left ventricle at physiological pressure if the stents $F_{pullout}$ is less than the $F_{in\ \ vivo}$ (Mummert et al., 2013).

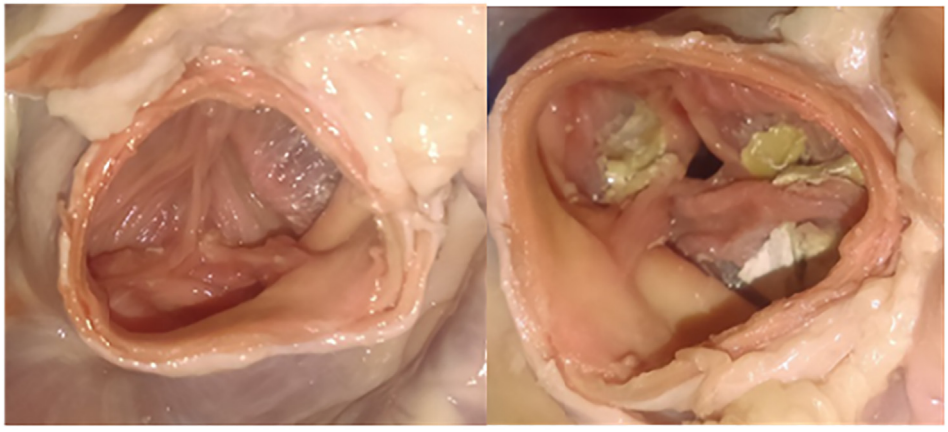

Fig. 3. (a) Uncalcified and (b) calcified porcine aortic valve.

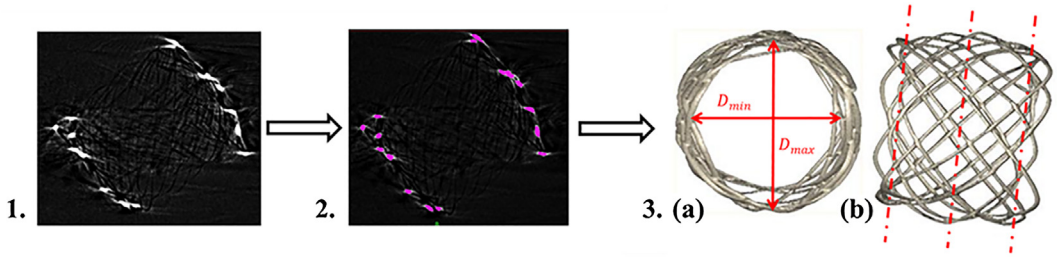

Fig. 4. Creation of the stent geometry from (a) the MSCT scan of the stent, (b) depicts segmentation of the stent using Mimics 14.1 to threshold the MSCT scans, and (c) reconstruction of the stent post-deployment in calcified porcine aortic root, measurements were taking of the maximum and minimum diameters at the top, middle and bottom of the stent.

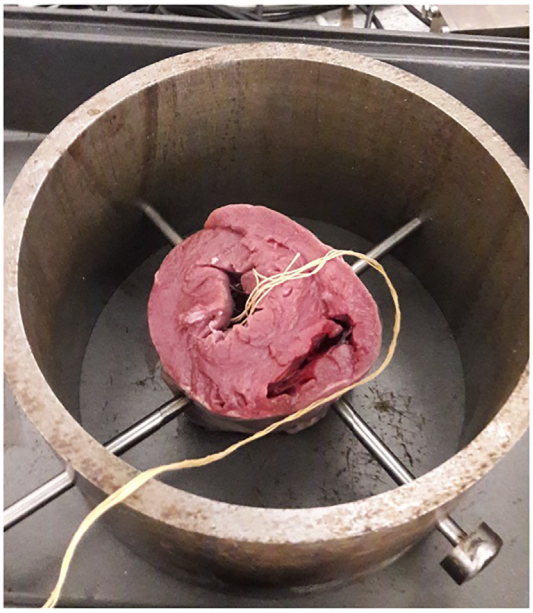

Fig. 5. (a) Porcine heart with apex dissected and pinned in place prior to pullout test.

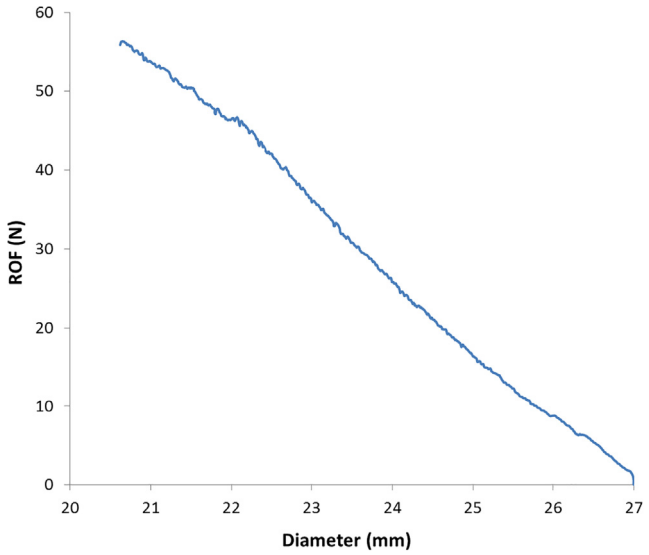

Fig. 6. Radial outward force (N) versus diameter (mm) for the stent.

2.3. Statistical analysis

Data were analysed using (GraphPad Prism, GraphPad Software, La Jolla California USA). Two-tailed Student's t-tests were used to determine statistical differences between the non-calcified and calcified groups for eccentricity, radial force, pull-out force and coefficient of friction. Statistical significance was defined as $p \leq 0.05$.

3. Results

3.1. Radial force

The radial force test was performed at 37 °C, the radial force test data illustrated in Fig. 6 shows the radial force versus diameter for the given braided stent geometry. It was found that crimping the stent from a diameter of 27 mm to a diameter of 20 mm lead to an approximate increase of 55 N in the radial force exerted by the stent.

The maximum diameters measured from the stent when deployed into the non-calcified porcine hearts' roots were found to be in the range of 23.38 ± 1.11 mm, with minimum diameters equal to 22.82 ± 1.37 mm. This can be compared to maximum and minimum diameters of 24.39 ± 0.91 mm and 23.11 ± 1.20 mm respectively measured from the stent when it was deployed in the calcified porcine aortic roots. This gave average diameters of 23.10 ± 1.05 mm (non-calcified group) and 23.75 ± 1.24 mm (calcified group). There was no significant difference found in the diameter of the stents between the two groups ($p = 0.51$).

The radial force data was extrapolated from Fig. 6, based on the average diameter of the stent. It was found that the radial force exerted on the aortic root ranged from 19.31 to 38.79 N in the non-calcified hearts versus 13.20–38.36 N for the calcified hearts. No statistical difference was found in the radial force of both groups with the radial force averaging 32.71 ± 11.62 N for the non-calcified and 26.85 ± 11.08 N for the calcified group ($p = 0.53$).

3.2. Stent eccentricity

Stent eccentricity was measured using Eq. (2) from the maximum and minimum diameters of the stent. It was found that the eccentricity of the stent ranged from 0.01 to 0.037 in the non-calcified roots. This compared to eccentricities of 0.034–0.067 for the calcified roots. There was found to be a significant difference ($p = 0.049$) in the eccentricities between the two groups, whereby the eccentricity in the stent when calcification was present (0.053 ± 0.015) was significantly greater than that without calcification (0.024 ± 0.014).

3.3. PullOut test and friction coefficient

The average stent pullout force was 2.84 ± 1.55 N for the non-calcified roots, which compared to a stent pullout force of

Table 1
Results of the tissue-stent interaction for the non-calcified aortic roots.

	Eccentricity	Radial force	Pull out	Friction coefficient
Test 1	0.037	38.790	1.400	0.036
Test 2	0.010	19.318	2.630	0.136
Test 3	0.026	40.025	4.479	0.112
Average	0.02	32.71	2.84	0.09
Standard deviation	0.01	11.62	1.55	0.05

Table 2
Results of the tissue-stent interaction for the calcified aortic roots.

	Eccentricity	Radial force	Pull out	Friction coefficient
Test 1	0.050	23.057	5.704	0.346
Test 2	0.067	32.765	7.985	0.205
Test 3	0.034	13.201	6.733	0.510
Test 4	0.061	38.360	13.931	0.363
Average	0.05	26.85	8.59	0.36
Standard Deviation	0.01	11.08	3.68	0.12

8.58 ± 3.68 N for the calcified roots. There was a significant increase in the force required to dislodge the stent in the calcified group when compared to the non-calcified group ($p = 0.045$). The coefficient of friction was calculated using Eq. (3) and found to be 0.09 ± 0.05 (non-calcified) and 0.36 ± 0.12 (calcified). The presence of calcification lead to a significant increase in the coefficient of friction between the stent and the aortic root ($p = 0.018$) (see Tables 1 and 2).

The predicted *in vivo* pullout force was calculated using Eq. (4), this represents the maximum force predicted to be acting on the valve stent *in vivo*. A physiological pressure gradient of 100 mmHg was used to represent a patient with stage 2 hypertension and thus represent a 'worst case scenario' criteria (Mummert et al., 2013) and the maximum diameter of the stent were used in calculating the max force acting on the stent *in vivo*. It was found that F_{invivo} was calculated as 5.72 N for the non-calcified root whereas this was 6.23 N for the calcified aortic root.

4. Discussion

This study developed an *in vitro* experimental model to represent a calcified aortic root and applied this model to determine the pullout and radial expansion forces of a TAV stent, and the coefficient of friction between the stent and aortic root. It was found that, in the presence of calcification, the coefficient of friction was significantly increased (0.35 ± 0.015) compared to that of non-calcified valves (0.09 ± 0.05). This increase in friction leads to an increase in the pullout force required to dislodge the stent. While it has been previously proposed that calcification helps to secure the TAV stent in position (Cribier et al., 2002), this study provides the first quantitative experimental data to provide evidence in support of the role of calcification for tissue-stent interaction. Furthermore, we report that the range of stent eccentricities increased (0.03–0.07) in calcified roots, compared to that of non-calcified roots (0.01–0.04). Moreover, we report that in the presence of calcification the pullout force required to dislodge the stent was higher than the predicted *in vivo* force, which implies that the stent would be unlikely to migrate into the left ventricle *in vivo*.

It must be taken into account that both calcifications and arterial stiffness have an impact on the stent-tissue interaction (Russ et al., 2013; Tzamtzis et al., 2013). In this study we have only examined the effect of calcification; however, stiffening of the tissue due to age was not examined. It must also be noted that calcification can cause tissue degradation and disrupt the structural integrity of the tissue matrix in the surrounding regions. However, tissue alteration due to calcification and disease progression was not included in this study. Nevertheless, the focus of this study is to examine the impact of calcification on the tissue stent interaction. Therefore, the tests are carried out only changing the attachment of calcification to the valve. Throughout this study authors refer to the coefficient of friction as the ratio between the pullout and the radial force, this relationship was previously defined in the study of Mummert et al. (Mummert et al., 2013). However, it must be noted that in the presence of calcification this relationship is somewhat simplified as any "hooking" of calcification between the stent cells is also included in this interaction. Nevertheless, this is this first study to approximate the impact of calcification on the coefficient of friction and demonstrate the role of calcification in securing the valve in place. It was also assumed that the glue does not interact with the stent but only serves to hold the calcification in place on the tissue. The lack of material properties available in literature restricts comparison of the *in vitro* experimental calcification model to properties of physiological calcification. However, by our μCT analysis, the density of the artificial calcification was within in the range of Hounsfield units of aortic calcification and as such was considered appropriate for the purposes of this study. Furthermore, there was some variation in the shape and size of calcifications applied to the leaflets and only one volume of calcification was tested in this study. However, these were evenly distributed across the leaflets and the total volume of calcification was kept constant. It must also be considered that this is a static analysis, which did not account for the dynamic motion of the aortic root, and tissue remodelling or growth was not considered. As the radial expansion force was determined experimentally it was assumed that the tissue responses were passive material properties (Mummert et al., 2013). Further to this, it must be noted that the radial force can only be approximated, particularly in eccentric deployment conditions. For this reason, we take the minimum and maximum diameter along three different sections of the stent with the goal of getting an approximation of the average radial force acting across the stent as whole. It must be noted that a similar method was used in determining the force exerted by stent in the previous quantification of the tissue stent interaction (Mummert et al., 2013) and radial force testing is an ISO standard test that is required to be carried out on all vascular stents and does not take into account eccentricity. Human tissue was not used in this study due to limited availability and porcine hearts may not be representative of human tissue. It must be noted that a commercial stent was not used in this study. Moreover, in this study the stent was used as a gauge to measure radial force, following a previous approach (Mummert et al., 2013) and it must be noted, that once the valve stent is fully expanded, there will be no further increase in diameter or associated radial force. However, in this study the stent was not fully expanded in any of the cases and the radial forces recorded across both groups (29.36 ± 10.78 N) were within the range predicted by computational modelling of the commercial self-expanding CoreValve stent (12.6–44 N in aortic annuli ranging from 20 to 23 mm) (Tzamtzis et al., 2013).

It was found that the average stent diameter did not significantly differ between the two groups, which suggests that the stent diameter may be more strongly influenced by the geometry of the aortic root. However, there was a significant increase in eccentricity in the calcified group. Interestingly, clinically it has been shown that valves are may exhibit higher eccentricities in higher calcified roots (Cavero et al., 2012; Zegdi et al., 2008).

The results of the study found that the coefficient of friction in a non-calcified root to be 0.09 ± 0.05, with stent eccentricities ranging from 0.01 to 0.04 N. This is in agreement with previously

reported findings of a coefficient of friction of 0.1 ± 0.01 and eccentricities of (0–0.03) in a study examining the tissue-stent interaction in a non-calcified root (Mummert et al., 2013). We report for the first time that in the presence of calcification the coefficient of friction significantly increases ($p = 0.02$), while, also verifying that calcification significantly increases the stent eccentricity ($p = 0.049$). The increase in friction (0.36 ± 0.12) due to the presence of calcification lead to a significant increase in the pullout force ($p = 0.045$), which suggest that that the stent was more secure in the presence of calcification. Comparing the pullout force to the predicted *in vivo* pullout force it was found that an average pullout force of 2.84 N was required to dislodge the stent in the non-calcified root where the maximum force acting to dislodge the stent *in vivo* was predicted as 5.72 N suggesting the stent would dislodge under *in vivo conditions*. This compares to an average pullout force of 8.59 N for the calcified root where the max force acting on the stent *in vivo* was calculated as 6.23 N. This suggests that the stent would not dislodge *in vivo* in the presence of calcification. Both $F_{in\,vivo}$ forces are in close agreement with the range of axial forces previously predicted computationally to act on the TAV *in vivo* (5.8–6.1 N) (Sun et al., 2010). The results of this study suggest that the stent is more secure within the aortic root in the presence of calcification. These results are in agreement with a study by Cribier et al, which reported that TAV stents deployed in non-calcified roots are associated with early migration and it was proposed that this migration arose due to the lack of calcification securing the valve in place (Cribier et al., 2002). An increase in pullout force can be explained by an increase in the radial force and/or an increase in the coefficient of friction (Eq. (3)). As there was no statistical difference in the radial force of both groups, we propose that the valve stent is secured in place due to the increase in friction between the stent and the aortic root. Although there was a change in eccentricity. there was no significant difference in the average diameter between the calcified and non-calcified cases. Thus we deduce that the diameter of the stent is predominantly affected by the diameter of the aortic root and the amount of aortic root recoil. This lack of change in average diameter would explain the fact that no significant increase is observed in the radial force between the two groups. However, it must be noted that *in vivo* the stiffening of the tissue in the aortic root due to age may lead to a lower degree of recoil of the aortic tissue, smaller stent diameters and an increased radial force compared to that of healthy tissue. The results reported here provided an important insight into the role of the friction provided by calcification nodules for preventing stent migration.

It has previously been shown that the presence of calcification can lead to aortic root rupture, and there is at higher risk in patients with more highly calcified roots (Cavero et al., 2012; Zegdi et al., 2008). However, the role of calcification in securing the stent in place, particularly in patients with higher levels of calcification must be considered. The results of this study show that ability of calcification to anchor the stent allows for a lower radial force required to secure the stent in place, which can thereby reduce the risk of rupture. This should be further considered with regard to patient-specific sizing and stent design. Further to this, the impact of a higher coefficient of friction in finite element modelling and its impact on the biomechanical response is something that should be further investigated.

In conclusion, we have developed the first *in vitro* model of aortic calcification and have shown that calcification significantly impacts the friction between the aortic tissue and TAV stent and the force required to dislodge the stent and stent eccentricity. This study demonstrates for the first time the impact of calcification on the friction between the aortic tissue and TAV stent, which shows that calcification, secures the stent in place in the aortic root. The impact of calcification should be given further consideration in TAVI procedures, as although higher levels of calcification increase the likelihood of aortic root rupture whereas there is a lesser need for higher radial forces to secure the stent in place. The impact of calcification and the degree of calcification of a given patient is something that should be further considered in device selection and design. Further to this, the coefficient of friction should be carefully considered in future biomechanical models of deployment of the TAV into an aortic root including the native calcified leaflets.

5. Disclosures

None.

6. Conflict of interest statement

Funding: This study was funded by an Irish Research Council Enterprise Partnership Scheme Postgraduate Scholarship 2014 in collaboration with Boston Scientific (EPSPG/2014/120), and grants from National University of Ireland Travelling Studentship 2015.

Conflict of Interest: Orla M. McGee and Professor Laoise M. McNamara are collaborating with Boston Scientific under an Irish Research Council Enterprise Partnership Scheme Postgraduate Scholarship. Wei Sun owns stock in Dura LLC, Storrs, CT.

References

Auricchio, F., Conti, M., Morganti, S., Reali, A., 2014. Simulation of transcatheter aortic valve implantation: a patient-specific finite element approach. Comput. Methods Biomech. Biomed. Eng. 17, 1347–1357.

Block, P.C., 2010. Leaks and the "great ship" TAVI. Catheter Cardiovasc. Interv. 75, 873–874.

Capelli, C., Bosi, G.M., Cerri, E., Nordmeyer, J., Odenwald, T., Bonhoeffer, P., Migliavacca, F., Taylor, A.M., Schievano, S., 2012. Patient-specific simulations of transcatheter aortic valve stent implantation. Med. Biol. Eng. Comput. 50, 183–192.

Cavero, M.A., Goicolea, J., García-Montero, C., Oteo, J.F., 2012. Prognostic implications of asymmetric morphology in transcatheter aortic Valve implantation: a case report. Revista Española de Cardiología (English Edition) 65, 104–105.

Cribier, A., Eltchaninoff, H., Bash, A., Borenstein, N., Tron, C., Bauer, F., Derumeaux, G., Anselme, F., Laborde, F., Leon, M.B., 2002. Percutaneous transcatheter implantation of an aortic valve prosthesis for calcific aortic stenosis. First Human Case Descrip. 106, 3006–3008.

Dwyer, H.A., Matthews, P.B., Azadani, A., Ge, L., Guy, T.S., Tseng, E.E., 2009. Migration forces of transcatheter aortic valves in patients with noncalcific aortic insufficiency. J. Thorac. Cardiovasc. Surg. 138, 1227–1233.

Généreux, P., Head, S.J., Hahn, R., Daneault, B., Kodali, S., Williams, M.R., van Mieghem, N.M., Alu, M.C., Serruys, P.W., Kappetein, A.P., Leon, M.B., 2013. Paravalvular leak after transcatheter aortic valve replacement the new Achilles' Heel? A comprehensive review of the literature. J. Am. College Cardiol. 61, 1125–1136.

Gooley, R.P., Cameron, J.D., Meredith, I.T., 2015. Assessment of the geometric interaction between the lotus transcatheter aortic valve prosthesis and the native ventricular aortic interface by 320-multidetector computed tomography. JACC: Cardiovasc. Interv. 8, 740–749.

Gunning, P.S., Vaughan, T.J., McNamara, L.M., 2014. Simulation of self expanding transcatheter aortic valve in a realistic aortic root: implications of deployment geometry on leaflet deformation. Ann. Biomed. Eng. 42, 1989–2001.

Haensig, M., Rastan, A.J., 2012. Aortic valve calcium load before tavi: is it important? Annals Cardiothorac. Surg. 1, 160–164.

Leber, A.W., Kasel, M., Ischinger, T., Ebersberger, U.H., Antoni, D., Schmidt, M., Riess, G., Renz, V., Huber, A., Helmberger, T., Hoffmann, E., 2013. Aortic valve calcium score as a predictor for outcome after TAVI using the CoreValve revalving system. Int. J. Cardiol. 166, 652–657.

Leon, M.B., Smith, C.R., Mack, M., Miller, D.C., Moses, J.W., Svensson, L.G., Tuzcu, E. M., Webb, J.G., Fontana, G.P., Makkar, R.R., Brown, D.L., Block, P.C., Guyton, R.A., Pichard, A.D., Bavaria, J.E., Herrmann, H.C., Douglas, P.S., Petersen, J.L., Akin, J.J., Anderson, W.N., Wang, D., Pocock, S., 2010. Transcatheter aortic-valve implantation for aortic stenosis in patients who cannot undergo surgery. New England J. Med. 363, 1597–1607.

Masson, J.-B., Kovac, J., Schuler, G., Ye, J., Cheung, A., Kapadia, S., Tuzcu, M.E., Kodali, S., Leon, M.B., Webb, J.G., 2009. Transcatheter aortic valve implantation review of the nature, management, and avoidance of procedural complications. JACC: Cardiovasc. Interv. 2, 811–820.

McGee, O.M., Gunning, P.S., McNamara, A., McNamara, L.M., 2018. The impact of implantation depth of the Lotus™ valve on mechanical stress in close proximity to the bundle of his. Biomech. Model. Mechanobiol.

Morganti, S., Brambilla, N., Petronio, A.S., Reali, A., Bedogni, F., Auricchio, F., 2016. Prediction of patient-specific post-operative outcomes of TAVI procedure: the impact of the positioning strategy on valve performance. J. Biomech.

Morganti, S., Conti, M., Aiello, M., Valentini, A., Mazzola, A., Reali, A., Auricchio, F., 2014. Simulation of transcatheter aortic valve implantation through patient-specific finite element analysis: two clinical cases. J. Biomech. 47, 2547–2555.

Mummert, J., Sirois, E., Sun, W., 2013. Quantification of biomechanical interaction of transcatheter aortic valve stent deployed in porcine and ovine hearts. Ann. Biomed. Eng. 41, 577–586.

Reinders, A., de Vries, C.S., Joubert, G., 2015. Pre-interventional assessment and calcification score of the aortic valve and annulus, with multi-detector CT. Transcatheter Aortic Valve Implantation (TAVI) Using the Medtronic CoreValve.

Russ, C., Hopf, R., Hirsch, S., Sundermann, S., Falk, V., Szekely, G., Gessat, M., 2013. Simulation of transcatheter aortic valve implantation under consideration of leaflet calcification. Conf. Proc. IEEE Eng. Med. Biol. Soc. 2013, 711–714.

Schoenhagen, P., Hill, A., Kelley, T., Popovic, Z., Halliburton, S.S., 2011. In vivo imaging and computational analysis of the aortic root. Application in clinical research and design of transcatheter aortic valve systems. J. Cardiovasc. Transl. Res. 4, 459–469.

Seiffert, M., Fujita, B., Avanesov, M., Lunau, C., Schön, G., Conradi, L., Prashovikj, E., Scholtz, S., Börgermann, J., Scholtz, W., Schäfer, U., Lund, G., Ensminger, S., Treede, H., 2016. Device landing zone calcification and its impact on residual regurgitation after transcatheter aortic valve implantation with different devices. Euro. Heart J. – Cardiovasc. Imaging 17, 576–584.

Sturla, F., Ronzoni, M., Vitali, M., Dimasi, A., Vismara, R., Preston-Maher, G., Burriesci, G., Votta, E., Redaelli, A., 2016. Impact of different aortic valve calcification patterns on the outcome of transcatheter aortic valve implantation: a finite element study. J. Biomech.

Sun, W., Li, K., Sirois, E., 2010. Simulated elliptical bioprosthetic valve deformation: implications for asymmetric transcatheter valve deployment. J. Biomech. 43, 3085–3090.

Tzamtzis, S., Viquerat, J., Yap, J., Mullen, M.J., Burriesci, G., 2013. Numerical analysis of the radial force produced by the Medtronic-CoreValve and Edwards-SAPIEN after transcatheter aortic valve implantation (TAVI). Med. Eng. Phys. 35, 125–130.

Vad, S., Eskinazi, A., Corbett, T., McGloughlin, T., Vande Geest, J.P., 2010. Determination of coefficient of friction for self-expanding stent-grafts. J. Biomech. Eng. 132. 121007-121007.

Vahanian, A., Alfieri, O., Al-Attar, N., Antunes, M., Bax, J., Cormier, B., Cribier, A., De Jaegere, P., Fournial, G., Kappetein, A.P., Kovac, J., Ludgate, S., Maisano, F., Moat, N., Mohr, F., Nataf, P., Piérard, L., Pomar, J.L., Schofer, J., Tornos, P., Tuzcu, M., van Hout, B., Von Segesser, L.K., Walther, T., 2008. Transcatheter valve implantation for patients with aortic stenosis: a position statement from the European Association of Cardio-Thoracic Surgery (EACTS) and the European Society of Cardiology (ESC), in collaboration with the European Association of Perc.... Eur. Heart J. 29, 1463–1470.

Wang, Q., Kodali, S., Primiano, C., Sun, W., 2015. Simulations of transcatheter aortic valve implantation: implications for aortic root rupture. Biomech. Model. Mechanobiol. 14, 29–38.

Wang, Q., Sirois, E., Sun, W., 2012. Patient-specific modeling of biomechanical interaction in transcatheter aortic valve deployment. J. Biomech. 45, 1965–1971.

Wendt, D., Muller, W., Hauck, F., Thielmann, M., Wendt, H., Kipfmuller, B., Vogel, B., Jakob, H., 2009. In vitro results of a new minimally invasive aortic valve resecting tool. Eur. J. Cardiothorac. Surg. 35, 622–627. discussion 627.

Zegdi, R., Ciobotaru, V., Noghin, M., Sleilaty, G., Lafont, A., Latremouille, C., Deloche, A., Fabiani, J.N., 2008. Is it reasonable to treat all calcified stenotic aortic valves with a valved stent? Results from a human anatomic study in adults. J. Am. College Cardiol. 51, 579–584.